01/11/2011
Biochim Biophys Acta-Bioenergetics. 2012 Aug;1817(8):1152-63. doi: 10.1016/j.bbabio.2012.01.008

Review

Photosynthetic cytochrome *c*550

Mercedes Roncel[a*], Diana Kirilovsky[b], Fernando Guerrero[a,c], Aurelio Serrano[a] and José M. Ortega[a]

[a]Instituto de Bioquímica Vegetal y Fotosíntesis, Universidad de Sevilla-CSIC, Américo Vespucio 49, 41092-Sevilla, Spain. [b]Commissariat à l'Énergie Atomique, Institut de Biologie et Téchnologies de Saclay (iBiTec-S), 91191 Gif-sur-Yvette, France, and Centre National de la Récherche Scientifique, URA 2096, 91191 Gif-sur-Yvette, France. [c]Present adress: Bioenergy Group, Molecular Plant Biology Unit, Department of Biochemistry and Food Chemistry, University of Turku, Tykistökatu 6B, Biocity 4th Floor, 20520, Turku, Finland

*Author for correspondence:

Mercedes Roncel

Instituto de Bioquímica Vegetal y Fotosíntesis, Universidad de Sevilla-CSIC, Américo Vespucio 49, 41092-Sevilla, Spain

Tel: 34 954 489525

Fax: 34 954 460065

E-mail: mroncel@us.es

Keywords: Cytochrome *c*550; Cyanobacteria; Diatoms; Photosystem II; *psb*V gene product; Red algae

Contents

Abbreviations: cyt, cytochrome; CP43, 43 kDa chlorophyll-binding protein in PSII; DAD, 2,3,5,6-tetramethyl-1,4-phenylenediamine or diaminodurol; D_1/D_2, homologous PSII reaction center core proteins; E_h, equilibrium redox potential; E_m, midpoint redox potential; EPR, electron paramagnetic resonance spectroscopy; OEC, oxygen evolving complex; P680, primary electron donor in PSII; PSI, photosystem I; PSII, photosystem II; Q_A/Q_B, redox-active quinones bound to PSII; RR, resonance raman; TMH, transmembrane alpha helix

1. Introduction

Cytochromes are hemoproteins with redox activity that function in a variety of electron transport processes ranging from aerobic respiratory chains to photosynthesis and reductive inorganic nutrient assimilation. Depending on the nature of their heme group, several classes of cytochromes can be distinguished [1]. *C*-type cytochromes, a widespread class of cytochromes, can be defined as having one or several hemes *c*, bound to the protein moiety by two (or rarely one) thioether bonds generated by reaction of thiol groups of cysteine residues with vinyl groups of the heme [2]. These cysteine residues almost always are found in the consensus heme *c* binding sequence CXXCH where X denotes any residue and H is one of the His axial ligand to heme iron. Almost any residues (except cysteine) may be found in the XX positions; very rarely there are three or four residues between the two cysteine residues [3]. In *c*-type cytochromes, the fifth ligand of the heme iron atom is always a histidine. A nitrogen atom of a histidine residue or a sulfur atom of a methionine residue fills the sixth ligand position of the heme iron atom [2].

Cytochrome *c*550 (cyt *c*550), encoded by the *psbV* gene, is a cytochrome with a molecular mass of ~ 15 kDa bearing a covalently bound heme-group protein [4, 5, 6]. Cyt *c*550 presents a bis-histidine heme coordination which is very unusual for monoheme *c*-type cytochromes. The only other known structure of bis-histidinyl coordination in a monoheme cyt *c* fold is found in a domain of the nitrite reductase complex cyt *cd*1, from *Thiosphaera panthotropha* [7]. Therefore, cyt *c*550 is the first structural example of a monodomain, monoheme soluble cyt *c* with bis-histidinyl axial coordination [8].

Although it was initially isolated as a soluble protein, currently it is clearly established that it is an extra-membrane component of the PSII complex in cyanobacteria and some eukaryotic algae, as red and brown algae [9, 10, 11]. In PSII, the cyt *c*550 with the other extrinsic proteins stabilizes the binding of Cl^- and Ca^+ to the oxygen evolving complex and

protects the Mn_4Ca cluster from attack by bulk reductants [5, 6, 11, 12]. The role (if there is one) of the heme of the cyt c550 is unknown. The low midpoint redox potential (E_m) of the purified soluble form (from -250 to -314 mV) [13, 14, 15, 16] is incompatible with a redox function in PSII. However, more positive values for the E_m have been obtained for the cyt *c*550 bound to the PSII [16, 17]. A recent work has showed an E_m value of +200 mV for cyt *c*550 [18].

These data raised the possibility of a redox function for this protein in electron transfer in PSII [18]. Despite the long distance (22 Å) between cyt *c*550 and the nearest redox cofactor (Mn_4Ca cluster) [19], an electron transfer reaction between these components is possible [18]. This reaction, even with a very slow rate (ms-s time scale) relative to charge separation events, could be potentially significant relative to the lifetime of reversible charge accumulation states in the enzyme (tens of seconds to minutes) [20]. Some kind of protective cycle involving a soluble redox component in the lumen has also been proposed [18].

The aim of this article is to review previous studies done on cyt *c*550 and to consider its function in the light of the new results obtained in recent years. The emphasis is on the physical properties of the heme and its redox properties. For earlier reviews on cyt *c*550 see articles by Krogmann [21, 22]. Several reviews have been published on photosynthetic soluble cytochromes including cyt *c*550 [5, 23]. Recent articles on the three-dimensional (3-D) structure of PSII contain also information on the structure of PSII-bound cyt *c*550 [19, 24, 25, 26, 27]. A number of reviews have been written about extrinsic proteins of PSII and contain information on cyt *c*550 [28, 29, 30].

2. Occurrence

Cyt *c*550 was initially found as a soluble protein in the cyanobacterium *Anacystis* (*A.*) *nidulans* [13] and later in *Microcystis* (*M.*) *aeruginosa*, *Aphanizomenon* (*A.*) *flos-aquae* [14]

and *Synechocystis* sp. PCC 6803 [15]. In the eighties, a membrane bound cytochrome with similar size, spectrum and redox properties was detected in detergent treated photosynthetic membranes from the cyanobacteria *Anabaena variabilis* and *Phormidium laminosum* [9, 31]. Later, a similar membrane-associated cytochrome in addition to the soluble form was obtained washing the thylakoids of *A. nidulans* with low ionic strength or with 1 M NaCl. However, these forms were distinct in their binding in ion-exchange chromatography and in EPR spectra [10, 32]. In the nineties, a PSII core complex purified from the thermophilic cyanobacterium *Synechococcus vulcanus* was described. This complex contained a stoichiometric amount of cyt *c*550 as one of the extrinsic components of cyanobacterial PSII [4, 33]. Based on its close interaction with the extrinsic 33- and 12-kDa proteins (*PsbO* and *PsbU*), it was concluded that cyt *c*550 is associated with PSII at the lumenal surface of the thylakoid membrane [11]. Nowadays, it is clearly established that cyt *c*550 is a component of the PSII complexes in cyanobacteria, which can be extracted by detergent or high salt treatments [9, 10, 33]. The three-dimensional structure of the PSII isolated from two different thermophilic cyanobacteria strains has confirmed that cyt *c*550 is stoichiometrically bound to the luminal PSII surface in the vicinity of the D1 and CP43 proteins and close to the oxygen-evolving complex [19, 24, 25, 26, 27, 34].

Cyt *c*550 has also been identified in the red algae *Cyanidium caldarium, Porphyra purpurea, Porphyridium cruentum* and *Cyanidioschyzon merolae* [14, 28, 35, 36, 37] and in the diatoms *Navícula pelliculosa* [38], *Phaeodactylum tricornutum* [39] and *Odontella sinensis* [40]. The presence of this protein in several eukaryotic algae has also been confirmed by detection of the *psbV1* gene in these organisms [35, 37, 40, 41, 42, 43, 44].

There is only one article in which cyt *c*550 has been detected in a green alga (*Bryopsis maxima*) by a spectrum assigned to this cytochrome [45]. No further confirmation has been

made by other authors and no cyt *c*550 protein sequence or *psbV* gene has been found for any green algae in any of the databases searched.

Sequence alignments and *psbV* gene distribution of cyt *c*550 among 39 different cyanobacterial genomes has been recenltly reported [23]. In the present review, we did a more extensive study on the distribution of this protein in different photosynthetic organisms using public databases and the Genbank database [htpp://www.ncbi.nlm.nih.gov]. About 90 organisms contain the *psbV* gene. Most of these organisms are cyanobacteria strains (57), but *psbV* is also present in different phylogenetic groups of photosynthetic eukaryotes (32) as Rhodophyta (or red algae) (10), Stramenopiles (or heterokonts) (17) and photosynthetic alveolates (9). It also appears in Glaucocystophyta (1), Haptophyta (2), Cryptophyta (2) and Rhizaria (1). A group of selected representatives are shown in Table 1.

Evolutionary relationships between the different photosynthetic organisms containing this protein were studied by using the alignment of all sequences available in database. A phylogenetic tree [46] that envisages these evolutionary relationships is presented in Figure 1. Cyanobacterial cyt *c*550 sequences constitute a well-defined cluster, arranged separately from the assembly of eukaryotic clusters which includes sequences of Glaucophyta, Rhodophyta and diverse photosynthetic protists bearing complex plastids of red algal ancestry (Dinophyta, Cryptophyta, Haptophyta, and Stramenopiles). These data are in agreement with the evolutionary history of these groups of photosynthetic eukaryotes, since Cryptophyta, Haptophyta, Stramenopiles and most photosynthetic alveolates (Chromerida and Dinophyta) are considered as evolutionary descendants of red algae. It is interesting to note that cell ultra-structural and molecular phylogenetic data strongly suggest that they originated by secondary endosymbiosis from rhodophycean ascestors engulfed by different fagotrophic eukaryotes [47]. In accordance with this, cyt *c*550 is also present in Glaucocystophyta, an early branching protist group of the Viridiplantae assembly, thus

suggesting an ancestral character of this redox protein. It was then probably lost during the subsequent evolution of the green photosynthetic lineage, after divergence of the green and red algae. In accordance with this, cyt *c*550 is also present in the Rhizarian euglyphid (tecated amoeba) *Paulinella chromatophora*, a phototrophic protist bearing a cyanobacterium-like organelle named chromatophore. This protist was recently reported as the only representative known so far of an incipient lineage of photosynthetic eukaryotes that underwent a primary endosymbiosis different from that of the Viridiplantae lineage (Chromatophore genome sequence of *Paulinella* sheds light on acquisition of photosynthesis by eukaryotes) [48].

Some cyanobacteria contain another gene called *psbV2* that gives a protein product with 44% identity to cyt *c*550. This homolog was found in both unicellular and filamentous cyanobacteria [23]. In *Thermosynechococcus (T.) elongatus* this gene is located between *psbV* and the gene *petJ* encoding cyt *c*6. PsbV2 shows homology with both proteins, being similar to PsbV in the heme binding region and to petJ in the C-terminal region. These data together with the position of the *psbV2* gene on the chromosome suggest that this protein was generated during evolution by gene duplication and posterior intergenic recombination [49]. It seems that *psbV2* is expressed in *T. elongatus* but in an amount corresponding to 1% as compared to cyt *c*550 [50]. PsbV2 lacks a second histidine residue for axial ligation to the heme; however, its EPR spectrum is typical for a Fe_{III} in a low-spin state. EPR and Raman spectra suggested that the sixth ligand could be a tyrosine [50]. Based on a structural model of PsbV2, Tyr 86 appeared to be the most likely sixth axial ligand to the heme [50]. The E_m of this cytochrome-like protein must be very low since dithionite was not able to reduce it. Its function is unknown, but it could participate in the stabilization of the OEC. In fact, PSII isolated from a *T. elongatus* mutant lacking this protein presented a slightig lower oxygen evolving activity than that isolated from the WT [D Kirilovsky, unpublished data].

3. Physical properties

3.1. UV-visible spectra

The UV-visible electronic absorption spectrum of the oxidized soluble cyt *c*550 presents a broad absorption band with maximum at 524.5 nm, a Soret band peaking at 405.7 nm and other maxima at 350 and 275 nm. Upon reduction with dithionite, typical absorption peaks appear at 550 (α-band), 522 (β-band) and 417 nm (γ or Soret band) [15, 17, 50, 51]. Most optical measurements of cyt *c*550 focus on the α component of the Q band at 550 nm; this transition has a moderate extinction coeficient, and the interference from the absorbance of other chromophores is relatively small in this region compared to the Soret region [36, 52, 53, 54]. Usually, the changes in the redox state of the soluble cyt *c*550 are measured from the reduced-minus-oxidized spectrum as the difference between the maximum absorbance at 550 nm and the absorbance at one of the isosbestic points at 530 or 560 nm.

The PSII-bound cyt *c*550 spectrum has also been measured as a reduced-minus-oxidized difference spectrum to remove the overwhelming contribution from the excess of strongly absorbing chlorophylls [16, 18]. Unfortunately, in PSII preparations there is another cytochrome associated with PSII, the cyt *b*559 (λ_{max} = 559 nm) which has an absorbance band that overlaps with the 550 nm cyt *c*550 signal. To avoid this interference, spectra in the α/β-bands region of both cytochromes have been recorded at different solution redox potentials. Taking into account that the main redox potential forms of cyt *b*559 in *T. elongatus* have E_m values significantly higher than cyt *c*550, the spectrum of cyt *c*550 can be easily distinguished by selective chemical oxidation/reduction and substrating of spectra of cyt *b*559 [16, 18]. Figure 2 shows a difference absorption spectrum of cyt *c*550 obtained by subtracting absolute spectra at two different solution redox potentials. Spectrum 1 (–300 mV minus +458 mV) clearly shows that PSII core complexes contain two different cytochrome components with absorption maxima in the α-band at 559 and 550 nm. The component with an absorption

maximum in the α-band at 559 nm was assigned to cyt *b*559 [16]. The component with an absorption maximum in the α-band at 550 nm that appeared between +55 mV and –300 mV (spectrum 2) can be assigned to cyt *c*550. Thus, the spectrum of the PSII-bound cyt *c*550 can be well recorded if cyt *b*559 is selectively reduced, which makes its absorption contribution in the α-band at 550 of the cyt *c*550 insignificant (Figure 2).

3.2. Electron paramagnetic resonance spectra

EPR spectroscopy has been used to observe the oxidized Fe (III) form of soluble and PSII-bound cyt *c*550, since it is a technique sensitive to changes in the coordination environment of metal ions with unpaired electrons. Typical EPR spectra for both soluble and PSII-bound forms from different cyanobacteria have been published by different authors [10, 15, 16, 17, 50, 52] and in both forms, the *g* values obtained are typical for a *c*-type low spin heme [17].

The g-values found (g_z 2.94, g_y 2.24 and g_x 1.49) in *T. elongatus* for the soluble cyt *c*550 [17, 16, 50] were quite similar to those found in *A. nidulans* (g_z 2.98, g_y 2.24 and g_x 1.46) [10, 50] and *Arthrospira (A.) maxima* (g_z 2.90, g_y 2.27 and g_x 1.54) [55, 50], but slightly differ from those measured in the isolated cyt *c*550 from *Synechocystis* sp. PCC 6803 (g_z 2.87, g_y 2.28 and g_x 1.57) [8, 15, 16, 17]. The differences in the g values are related to subtle differences in the geometry and the environment of the heme in the different cytochromes [50].

EPR spectral properties of PSII-bound cyt *c*550 have also been also studied. Vrettos et al. [17] used isolated PSII from *Synechocystis* oxidized with ferrycianide. In this type of preparations, EPR spectra of PSII display overlapping EPR signals from cyt *b*559 and cyt *c*550 since the *g* tensors of these cytochromes are very similar. To avoid this overlap in the EPR signals, the difference in reduction potentials between these cytochromes was exploited.

Considering that cyt *c*550 has a lower redox potential than cyt *b*559, the EPR signal arising primarily from cyt *c*550 has been obtained by reduction of the cyt *b*559 in the PSII preparation with sodium ascorbate [17]. The g-values found in *Synechocystis* for the PSII-bound cyt *c*550 (g_z 2.88, g_y 2.23 and g_x 1.50) [17] were similar to those of the soluble form. In contrast, the values obtained with isolated *T. elongatus* PSII were different (g_z 3.02, g_y 2.20 and g_x 1.45) [16] from those obtained in *Synechocystis* and from the *T. elongatus* soluble cyt *c*550. In this case, dark-adapted non-treated PSII were used for the measurements in darkness. Under these conditions, cyt *b*559 was mainly reduced and EPR silent [16]. The differences between the bound cyt *c*550 could be explained by a weaker binding of the cyt *c*550 to the *Synechocystis* PSII than to *T. elongatus* PSII. In this regard cyt *c*550 is more easily lost during PSII isolation in *Synechocystis* than in *T. elongatus* [50]. In such a conformation, cyt *c*550 would therefore have the EPR characteristics of the unbound state.

To evaluate the environment of a six-coordinate low-spin heme the crystal field parameters such as rhombicity (V/Δ) and tetragonality (Δ/λ) must be calculated from the EPR g values [56, 57, 58]. The calculated rhombicity appears higher in the soluble cyt *c*550 isolated from *Synechocystis* (V/Δ=0.62) than in that of *A. maxima* (V/Δ=0.60) or *T. elongatus* (V/Δ=0.54) and *A. nidulans* (V/Δ=0.54) [50]. A correlation was found between the rhombicity value and the geometry of the heme-axial ligands based on the known crystallographic structures of the soluble cyt *c*550 from *T. elongatus* (PDB: 1MZ4), *Synechocystis* (PDB: 1E29) and *A. maxima* (PDB: 1F1C) [50]. Previously, a linear correlation has been observed between the rhombicity parameter and the dihedral angle between the imidazole planes and the NA-Fe-NC direction of the porphyrin ring in model compounds with parallel bis-imidazole axial ligands [59]. Thus, a concomitant decrease of the coplanarity of the two imidazole rings of the histidines and of the rhombicity were expected [50]. The superimposition of the axial ligands of the three cyt *c*550 structures, using the heme prosthetic

group as the basis of the superposition showed that the distortion of the heme-axial ligands (i.e. the loss of the co-planarity of the imidazole rings and the increase in the dihedral angle between these imidazole rings and the NA-Fe-NC direction of the porphyrin) was greater in *T. elongatus* (lowest rhombicity) than in *A. maxima* and *Synechocystis* being the least distorted in *Synechocystis* cyt *c*550 (highest rhombicity) [50].

The comparison of the rhombicity values of the soluble cyt *c*550 with that of the PSII-bound cyt *c*550 deduced from its EPR spectrum ($V/\Delta=0.48$) [16] suggested that the binding of cyt *c*550 to PSII induces important distortions in the heme-axial ligands geometry producing structural changes in the heme vicinity [50]. These distortions could be in part at the origin of the differences in the redox properties of soluble and PSII-bound forms of cyt *c*550 [16]. A decrease in the rhombicity is in agreement with an increase in the E_m [50]. However, in the case of the cyt *c*550 the value of the E_m is principally related to the solvent exposure of the heme that is greater in the soluble cyt *c*550 (see also below) [16].

3.3. Resonance Raman spectra

Resonance Raman (RR) spectroscopy has been used to probe the heme group and the coordination environment of iron in cyt *c*550 by comparison with model heme complexes. Therefore, the RR spectra of cyt *c*550 excited with visible or near-ultraviolet excitations have provided information about the vibrational modes of the heme group with relatively high sensitivity and without any interference from the protein or the solvent [60, 61].

The RR spectra of the *c*-type cytochrome shows two regions of high- and low frequency [62] with several bands identified with vibrational modes of the heme group, which shifts in frequency and intensity when the heme structure is altered [63]. The low-frequency region of the RR spectrum (300–700 cm^{-1}) of the cyt *c*550 exhibits a pattern characteristic of the *c*-type cytochromes with a series of intense bands in the 340–420 cm^{-1} region [62, 64]

including the modes ν_8 and ν_{50} at 347 and 364 cm^{-1}, respectively. The high-frequency region (1300–1650 cm^{-1}) of the RR spectrum of the soluble form of cyt *c*550 is consistent with a six-coordinate low-spin ferric heme with bis-His axial ligation [17].

The ability to correlate the structure of a heme with its Raman spectrum has been well documented [65]. Several vibrational modes in the high-frequency portion of the RR spectrum have been assigned. The mode ν_4 at 1372 cm^{-1}, predominantly corresponds to C_α-N stretch [66] which is sensitive to the iron oxidation state changing from 1355 cm^{-1} in Fe (II) porphyrins to 1375 cm^{-1} upon oxidation to Fe (III). The position of this mode in cyt *c*550, therefore, serves as the oxidation state marker for the Fe (III) [17]. The skeletal modes ν_2, ν_3, ν_{10} and ν_{37} have been clearly identified at 1584, 1503, 1637 and 1601 cm^{-1}, respectively [62, 64]. An empirical equation has been found which relates the energies of high-frequency heme skeletal modes and the core size. Application of this core-size relationship to the previous skeletal modes ν_2, ν_3, ν_{10} and ν_{37} has resulted in a core size of 1.99 Å, for cyt *c*550, which is characteristic for a low-spin ferric heme [67]. It has been shown that high-frequency modes are sensitive to the planarity of the porphyrin [64]. The mode ν_{10} at 1637 cm^{-1} in cyt *c*550 suggests that the heme is ruffled as is usual for many *c*-type cytochromes [17]. The ligand-sensitive mode ν_{11} at 1566 cm^{-1} is also of interest. This mode, primarily a C_β-C_β stretch, is modulated according to the properties of the axial ligands. The appearance of ν_{11} at 1566 cm^{-1} is a clear indicator of bis-His axial coordination in cyt *c*550 [17].

In conclusion, considering previous RR data on various ferric cytochromes and heme model compounds, the high- and low-frequency regions of RR spectra of the cyt *c*550 are characteristic of a six-coordinated low-spin *c*-type heme with a bis-histidine axial ligation of the iron [58, 62, 64, 68]. The RR spectra of cyt *c*550 also indicate that the heme structure is not very different from most *c*-type cytochromes, and thus the structure of the heme does not account for its unusually low E_m [17].

3.4. Redox properties

The E_m of cyt *c*550 was initially measured in the soluble state of the protein in two species of cyanobacteria being unusually low for a *c*-type monoheme cytochrome. An E_m value at pH 7.0 (E_{m7}) of –260 mV was the first to be reported for purified cyt *c*550 from *A. nidulans* [13]. Cyt *c*550 from *M. aeruginosa* and *A. flos-aquae* were found to be reducible by sodium dithionite (E_{m7} = -420 mV), but not by sodium ascorbate (E_{m7} = +58 mV) [14]. Later, E_{m7} values from -280 mV to -314 mV were obtained for purified cyt *c*550 from the same species [10]. An E_{m7} of -250 mV was measured in the cyt *c*550 isolated from *Synechocystis* [15]. Finally, an E_{m6} value of -240 mV for the soluble form of cyt *c*550 from the thermophilic cyanobacterium *T. elongatus* PSII was determined [16]. The E_m was the same in the cyt *c*550 isolated as a soluble protein from whole cells or in that extracted from PSII complexes [16].

Using an electrochemical technique, a 150 mV more positive value ($E_{m7} \approx$ -100 mV) was measured in soluble *Synechocystis* cyt *c*550 adsorbed to an electrode surface. This higher value was attributed to the exclusion of water from the heme site due to the protein binding to the electrode [17]. It was proposed that the binding of cyt *c*550 to PSII would reduce the solvent exposure of the heme [17], and so an increase in the E_m value would be expected. The E_m for cyt *c*550 associated with PSII was not established until 2003 when using intact PSII core complex preparations from *T. elongatus*, an E_m value of -80 mV was obtained [16]. This value was significantly higher as compared to its soluble form after its extraction from PS II (-240 mV at pH 6). Moreover, while the E_m of the bound form was pH-independent, the E_m of the soluble form varied from -50 mV at pH 4.5 to -350 mV at pH 9-10 [16].

The redox potentials of proteins are usually determined by redox potentiometry which involves the use of redox mediators that are required to ensure redox equilibrium. It has been described that redox mediators at low ambient potentials modify the E_m of Q_A in PSII-enriched membranes [69]. The proposal that the presence of these mediators could lead to the

reduction of the Mn_4Ca cluster, the consequent loss of the Ca^{2+} and Mn^{2+} ions and conformational changes in PSII, led to believe that the E_m value obtained for cyt *c*550 may not reflect the E_m of the fully associated and active form of the PSII-bound cytochrome. In fact, an E_m value of +200 mV was recently obtained [18] for PSII-bound cyt *c*550 in highly active and intact core complex preparations of PSII from *T. elongatus*, when redox titrations were performed in the absence of redox mediators or in the presence of only one mediator (DAD). This value was about 300 mV more positive than that previously measured in the presence of mediators (E_m= -80 mV) [16]. Fig. 3 shows the E_m values obtained for PSII-bound form of cyt *c*550 after its extraction from PSII (A), in the presence of 14 mediators (B) and in the absence of redox mediators (C). A summary of the E_m values of cyt *c*550 measured to date is shown in Table 2.

How can one explain the difference of about 500 mV between the E_m of the bound and unbound states of cyt *c*550? The E_m of a cytochrome is influenced by several factors, such as surface exposure of the heme to the solvent, hydrogen bonding to the propionate oxygen atoms, hydrogen bonding of the imidazole ligands and to a lesser extent by factors like the planarity of the heme, the relative angle between the two imidazole ligands and the dihedral angle between the N1-Fe-N3 direction of the porphyrin ring and the axial imidazole ligands plane [70]. EPR spectroscopy experiments shown that the rhombicity calculated for the bound cyt *c*550 (V/D=0.48) is lower than that calculated for the unbound cytochrome (V/D=0.58). A decrease in the rhombicity is in agreement with an increase in the E_m. Nevertheless, owing to the large difference in the redox properties of the two states of cyt *c*550, it seems likely that the structural modifications detected by EPR would rather be a consequence than the cause of this dramatic redox change. The X-ray crystal structures of the soluble and PSII-bound cyt *c*550 have shown that a portion of the heme is solvent accessible in the soluble form [55] but oriented towards the membrane, facing the Mn-stabilizing protein and the luminal surface of

PSII when it is bound to PSII [26]. Thus, a significant increase in the E_m, due to a lower solvent accessibility [71, 72], would be expected in its *in vivo* location. Therefore, the difference between the low and high-potential cyt *c*550 forms is related to the more hydrophobic environment of the heme when the cyt *c*550 is strongly bound to the PSII [18].

In order to explain the different E_m values obtained for the bound cyt *c*550 when potentiometric redox titration were done in the present or in the absent of redox mediators (-80 versus +200 mV [18]), it has been proposed that redox mediators could trigger the reduction of a component of PSII which is sequestered and out of equilibrium with the medium: most likely the Mn_4Ca cluster [18]. This reduction could generate a conformational change in PSII inducing a partial disassociation of the cyt *c*550 that increase the solvent accessibility of the heme, thus lowering the E_m. It was suggested that the E_m of +200 mV obtained without redox mediators could be the physiological redox potential of the cyt *c*550 in intact PSII. This new value has opened the possibility of a redox function for cyt *c*550 in PSII [18].

4. Protein structure

4.1. Amino acid sequences

The amino acid sequences of cyt *c*550 from 90 organisms are available. Alignment of the sequences from 21 organisms representing different phylogenetic groups: cyanobacteria, Glaucocystophyta, Rhodophyta (or red algae), diatoms, Phaeophyta, Chromerida and Dinophyceae was performed (Table 3). To this end, the mature portions of the proteins, after eliminating the signal peptide sequence, and Cobalt Multiple Alignment Tool [htpp://www.ncbi.nlm.nih.gov] were used. The amino acids sequences of cyt *c*550 for these organisms were all retrieved from the Protein Knowledgebase Server [htpp://www.uniprot.org]. Identical, strongly and weakly similar residues were indicated by (*), (:) and (.), respectively. This table shows that there are two histidine residues in positions

41 and 92 and two cysteines, Cys37 and Cys40 that appear to be conserved in all sequences. These residues correspond to the heme attachment site CXXCH and the sixth ligand of the iron. Of the 137 positions describing the total sequence, twenty (Thr9, Phe33, Gly44, Thr46, Lys47, Leu54, Leu59, Ala62, Pro64, Leu72, Pro79, Tyr82, Asp83, Gly84, Pro93, Arg105, Asp111, Trp130, Gly131, Gly132) are completely conserved residues giving an overall identity conservation of 15%. The most highly conserved amino acids are predominantly found in the region close to the heme pocket.

4.2. Structural properties

Three crystallographic structures of the soluble form of the cyt *c*550 are available: isolated from *Synechocystis* (PDB: 1E29) [8], *A. maxima* (PDB: 1F1C) [55] and *T. elongatus* (PDB: 1MZ4) [50]. The three proteins show a similar overall folding, being predominantly alpha-helical with a short two-stranded β-sheet near the N-terminus, similar to other monoheme *c*-type cytochromes. A bis-histidine heme coordination previously proposed from EPR studies [10, 15], which is unusual for monoheme *c*-type cytochromes, has been confirmed. The 3-D structure of soluble cyt *c*550 from *T. elongatus* (Fig. 4A) shows the typical hydrophobic inner core of monoheme cyt *c*, with three helices (residues 22-42, 68-78, 108-126) forming a nest for the prosthetic group [8]. It also presents a fourth helical segment (55-61) in the N-terminal domain, similarly to what is found in cyt *c*5 and *c*6, further protecting the heme from solvent [8]. An anti-parallel β-sheet (residues 8-12 and 17-21) connected by a β-hairpin turn (residues 13-16) near the N-terminus was also observed. This is an unusual feature in a monoheme *c*-type cytochrome that is almost exclusively composed of α-structures [2].

All sequences analyzed present three conserved residues of cis-proline (Pro64, Pro79 and Pro93) which correspond to turns on the structure of the molecule at the end of one alpha helix [55]. Proline residue at position 93 orients its carbonyl oxygen to form a hydrogen bond with

the Nδ atom of the axial His92 heme ligand [51]. All soluble cyt *c*550 structures have similar comparable Fe-axial ligand distances. The polypeptide chain largely envelops the heme prosthetic group with the exception of the propionate D oxygen atoms, showing comparable amounts of the buried heme [55]. Comparison of the three structures also shows that the porphyrin rings and the propionate A presents a similar position in the three species while the propionate D is found in different orientations, the difference being up to approximately 45°.

Structural alignment is usually applied for the structural comparison of proteins with low sequence similarity, where evolutionary relationships between them cannot be easily detected by standard sequence alignment techniques. The minimal root mean square deviation (rmsd) of two aligned structures is the measure of the average distance between the atoms (usually the backbone atoms) of superimposed proteins, indicating their divergence from one another. Comparison of the three available structures of soluble cyt *c*550 shows that *T. elongatus* cyt *c*550 superimposes on *Synechocystis* cyt *c*550 with an rmsd of 1.0 Å (126 C_α atoms) and on *A. maxima* cyt *c*550 with an rmsd of 0.79 Å (128 C_α atoms) [50]. Cyt *c*550 from the thermophilic cyanobacteria *T. elongatus* contains more intramolecular hydrogen bonds than its mesophilic counterparts: 102 compared to 81 and 82 in *A. maxima* and *Synechocystis* cyt *c*550, respectively [50]. This observation agrees with the proposal that increased numbers of hydrogen bonds and ion pairs, additional helices, and shorter loops may play a role in the structural basis of thermostability [50, 73]. No other thermostability-enhancing structural differences could be detected by comparing the three structures.

To date, two crystallographic structures of PSII-bound cyt *c*550 are available. These have been obtained from *T. elongatus* (PDB: 1W5C; 2AXT; 3BZ2) [19, 25, 74] and *T. vulcanus* (PDB: 3ARC) [27]. The resolution of the 3-D structure of these two PSII-bound forms of cyt *c*550 has shown that the N-terminal helix seems to be important for the interactions with other PSII subunits [26, 34]. Figure 4B shows the structure of PSII-bound cyt *c*550 from *T.*

elongatus. It is noteworthy that two conserved residues, Thr46 and Lys47, are shielding the pyrrole A, D, and C rings of the heme [55] and seems to participate in the electrostatic interaction of the cytochrome with other components of the PSII. Lys47 is in the proximity of PsbC-Glu413 (Fig. 4B). The side chains of the two highly conserved hydrophobic amino acids, Leu54 and Leu59, which are located in a short alpha-helical region in the proximity of the propionate and facing the heme, probably contribute to keep the hydrophobicity in the heme pocket [55]. Another hydrophobic conserved amino acid is Ala62, which is found in the periphery of the cytochrome, next to Tyr82 and psbU-Arg39, hence suggesting an inter- and intra-molecular structural role [8, 55]. Gly44 and Gly84 are located in different turns of loops in the cyt *c*550 tertiary structure. Gly44 is at the end of the first alpha-helix, which is part of the nest for the localization of the heme group, in close proximity to the conserved Leu59. On the other hand, Gly84 is found at the turn of the loop formed by the polar residues Tyr82 and Asp83, which can be crucial in the contact with PsbU [8, 55]. Gly131 and Gly132 are highly conserved probably due to the importance of the flexibility of the C-terminus for the recognition and binding to PSII. Likewise, Trp130 may be important in keeping the structure of this C-terminus anchoring region. Between conserved residues, the positively charged Arg105 is in the "upper" part, probably contributing to the cyt *c*550 binding to the PSII by interacting with PsbC-Glu104 [55].

The N-terminus of PsbV points towards the loop region between TMH-e and the membrane-attached α-helix eC of D1 as well as to the α-chain of cyt *b*559 [75]. A two-stranded β-sheet (β1 and β2) is found near the N-terminus followed by α-helix (α1) in the neighbourhood of CP43 [75]. Close to the Fe^{2+} coordinating residue PsbV-His41, located on a short loop segment between α1 and α2 (Fig. 4B), an H-bond is formed from PsbV-Asn49 to CP43-Arg320 [75]. The α-helix (α3) is located in the N-terminal of the second antiparallel β-sheet (β3 and β4). The β3 and the short loop linking β3 and β4 is in contact with the N-

terminal part of PsbU [75]. The loop between β4 and α4 is close to ef (3) in the extended loop of CP43. PsbV-His92, coordinating the Fe^{2+} is located downstream of two short α-helices (α4 and α5). The C terminus of PsbV is in close vicinity (~8 Å) to the currently modelled C-terminus of PsbU [75].

The heme group of PsbV is well defined in the electron density, tilted by 62° to the membrane plane (angle between the heterocycle plane normal and the pseudo-C2 (Fe^{2+}) axis) and shielded from solvent by hydrophobic residues of PsbV and the extended lumenal domain of CP43 (Fig. 4B). Fe^{2+} is coordinated by PsbV-His41Nε and PsbV-His92Nε that is H-bonded with NδH to PsbV-Pro93 (2.7 Å) [75]. The hydrophobic environment of the heme and the proximity of charged residues from other PSII components (PsbC-Lys323) could modulate the heme redox properties [75]. The redox potential difference between bound and isolated PsbV (-240 mV and +200 mV, respectively at pH 6.0) [18] could be caused by the additional shielding of the heme group by CP43 in the bound state. In the structure of soluble cyt *c*550 the C-terminal region is highly disordered, whereas in the PSII-bound cyt *c*550 structure, it is stabilised upon binding to the complex and points towards the Mn_4Ca cluster. While the edge-to-edge distance from the heme to the manganese cluster (22 Å) may be too high to consider a direct electron transfer reaction, the residue PsbV-Lys134 is at a distance of 10.2 Å from the Mn1 of the Mn_4Ca cluster. This lysine 134, together with the two C-terminal tyrosine residues (PsbV-Tyr136 and PsbV-Tyr137) could have functional importance in possible electron transfer reactions involving the cyt *c*550 and the S states of the OEC [18].

It is not clear how cyt *c*550 binds to PSII, or if significant structural changes occur during the binding process. By analogy with other cytochromes that bind photosynthetic membrane complexes, like cyt *c*6 (in association with the PSI) and cyt *f* (in association with the cyt *b*6*f*) [76, 77] it is possible to speculate that the binding of the cyt *c*550 to PSII could be due to electrostatic and hydrophobic interactions. The distribution of charges on the surface of the

cyt *c*550 supports this hypothesis [78]. Furthermore, the last residues in the carboxy-terminus of the cyt *c*550 (-GGKVYY) are not resolved in the soluble structure, while they are visible in the crystals when cyt *c*550 is bound to PSII. This indicates that this region is much more flexible when the cytochrome is in its soluble form [79]. Furthermore, the B-factors of the atoms in the C-terminus together with the section from His41 to Ser51 (-HVGGITKTNPS-) are the lowest of the cyt *c*550 structure. These regions are located between the heme and the contact with the PSII (PsbU, CP43 and D1). The degree of conservation of several of these residues and the low flexibility shown in the crystal structures (indicated by low B-factors and the lack of resolution in the soluble form) may indicate that the regions mentioned are important in the recognition and attachment between cyt *c*550 and the PSII [78].

The resolution of the 3-D structure of soluble and PSII-bound cyt *c*550 forms has confirmed that these are similar with different conformations found for only few amino acid side chains located at the interface formed by cyt *c*550 with D1, CP43, and *Psb*U and the six C-terminal amino acids. The soluble cyt *c*550 (PDB: 1MZ4) superimposes on PSII-bound form (PDB: 3BZ2) with an rmsd of 0.3 Å for 131 Cα atom pairs [75].

Comparison with other bacterial *c*-type cytochromes has been made using structural alignment between soluble cyt *c*550 and the structures of other class I cytochromes. All of these cytochromes are very distantly related: cyt *c*550 superimposes on yeast cyt *c* [80] with an rmsd of 3.4 Å, on *Rhodobacter sphaeroides* cyt *c*2 [81] with an rmsd of 4.2 Å (over 281 backbone atoms), on *Rhodopseudomonas viridis* cyt *c*2 [82] with an rmsd of 3.5 Å (over 281 backbone atoms), and on *Pseudomonas* cyt *c*551 [83] with an rmsd of 3.5 Å (over 273 backbone atoms) [55].

Comparison with cyt *c*6 has also been reported [55]. Cyt *c*6 is a soluble *c*-type cytochrome which donates electrons to PSI in cyanobacteria and algae but not in higher plants. The examination of the sequences of these cytochromes recognized two regions of sequence

similarity in the two proteins. The cyt *c*550 sequence from residue 28 to residue 45 is similar to the sequence of residue 1 to residue 18 in cyt *c*6. This includes an alignment of the heme-binding sites of cyt *c*550 of residues 37 and 40 with cyt *c*6 at residues 10 and 13. Another region of similarity is at the carboxy terminus of the two proteins. It has been suggested that the gene for one of the proteins provided segments for the assembly of a gene for the second cytochrome [22]. The superimposed structures of cyt *c*550 and cyt *c*6 from *A. maxima* (over 263 backbone atoms) showed an rmsd of 0.7 Å, despite only 32% identity between their primary structures [55]. This structural comparison between the helical cores of both *A. maxima* cyt *c*550 and cyt *c*6 shows great similarity. The longest helical segments closely superimpose on the four helices of cyt *c*6. The fold of the two proteins in the vicinity of the first axial ligand (His40 in cyt *c*550, His18 in cyt *c*6) is strikingly similar [55]. Cyt *c*550 has 22 additional residues in the N-terminal. In part they form a short, two-stranded β-sheet that precedes the first helix and the CXXCH heme coordination sequence (residues 37-41; Table 3). A second major difference between the two structures is the insert in the primary structure of cyt *c*550 that is not found in cyt *c*6 (between residues 89 and 103). It contains the sixth axial ligand, His92. The insert lacks secondary structure with the exception of the turn formed by residues 102-104. The protein backbone conformation in the region adjacent to the sixth axial ligand (His92 in cyt *c*550, Met61 in cyt *c*6) in the two structures is quite dissimilar. These results thereby reinforce the idea that cyt *c*550 and cyt *c*6 are actually close relatives [55].

5. Function

Cyt *c*550 was initially identified as a soluble protein with an E_m of about -240 mV [13, 14] suggesting functions not related to PSII for this protein. Several non-photosynthetic roles have been proposed for cyt *c*550, mostly in anaerobic carbon and hydrogen metabolism [22, 84, 85] (summarized in Table 4). It was suggested that the cyt *c*550 was an endogenous cofactor of

cyclic photophosphorylation [86]. Since cyt *c*550 was abundant in cells grown on high levels of nitrate and was absent from cells grown on ammonia it was proposed that it could participate in the reduction of nitrate to ammonia [14]. Krogmann and Smith [21] suggested that the function of cyt *c*550 could be related to anaerobic disposal of electrons from carbohydrate reserves or fermentation to sustain an organism during prolonged dark and anaerobic conditions. A very low rate of cyt *c*550 enzymatic reduction using NADPH and the spinach ferredoxin: NADP oxidoreductase (FNR) was observed under anaerobic conditions. A modest increase in the rate of this cytochrome was observed when ferredoxin II from cyanobacteria was added to the reaction mixture. The specificity for ferredoxin II in the reduction of cyt *c*550 and the often coincident appearance of ferredoxin II and cyt *c*550 in cells experiencing dark, anaerobic conditions suggested that these proteins may link carbohydrate breakdown to disposal of electrons in a fermentative pathway [21]. The low E_m of this cytochrome was similar to that of cyt *c*3 of *Desulfovibrio desulfuricans* [2] and so it could have similar functions. A few unicellular cyanobacteria and diatoms experience dark, anaerobic conditions as a result of bloom formation. Under these conditions, they acquire an hibernation ability and the appearance of the low-potential cyt *c*550 facilitating perhaps one fermentation pathway would make sense [22].

In the nineties, it was clearly demonstrated that the cyt *c*550 is one of the extrinsic proteins of the cyanobacterial PSII [10, 33]. It was shown that cyt *c*550 was stoichiometrically bound to the PS II, activated oxygen evolving activity and allowed the binding of the 12 kDa protein, another extrinsic component of the cyanobacterial PSII involved in oxygen evolution [33, 4, 11]. Cyt *c*550 was thus suggested to play the same role as the other extrinsic proteins. By stabilising the neighbouring proteins and protecting the Mn cluster from external reductants, it stabilizes the oxygen-evolving complex [12, 5]. Studies on the phenotype of the cyt *c*550-less mutant (ΔPsbV) and the cyt *c*550-less and 12 kDa protein-less double mutant

(ΔPsbV-ΔPsbU) of *Synechocystis* showed that both the cyt *c*550 and the 12 kDa protein stabilize the binding of the Ca^{2+} and Cl^- ions which are essential for the oxygen-evolving activity of PSII, in a manner analogous to the extrinsic 17 and 24 kDa polypeptides of higher plants [6, 49, 87]. Mutations of the axial ligand His-92 of cyt *c*550 to methionine or cysteine changed the E_m by +125 mV or -30 mV, respectively. Nevertheless, the activity of this mutated PSII in cells from *T. elongatus* was not modified, suggesting that under normal growth conditions the E_m of cyt *c*550 is not important for PSII function [52].

Since then, all the studies about the role of the cyt *c*550 have been related to its function in the PSII. However, it is still possible that two different populations of cyt *c*550 are present in cyanobacterial cells: one bound to the PSII and the second one soluble in the cytoplasm or in the lumen. EPR spectra of the cyt *c*550 recorded using whole *T. elongatus* cells suggested the presence of a significant concentration of soluble cyt *c*550 in cells: the g_x value observed in whole cells corresponded to the isolated cyt *c*550 with a shoulder that could be from the bound cyt *c*550 [52]. It was calculated that the soluble fraction could represent between 40 to 60% of the bound population. The role and cellular localization of the soluble cyt *c*550 is still unknown. However, the fact that the N-terminal amino-acid sequence of both cyt *c*550 populations was "AELTPE" indicates the loss of the 26 amino acids transit sequence also in the soluble fraction, and suggests a localization of this fraction in the lumen and not in the cytoplasm as suggested by its very low E_m [52]. A summary of the different functions proposed for cyt *c*550 is shown in Table 4.

Since the E_m of a cytochrome is one of the key parameters for elucidating its function, the discovery that the E_m of the PSII-bound cyt *c*550 is +200-215 mV opens the possibility that it plays a redox function [18]. Although the change of the E_m of the cyt *c*550 by replacing one of the histidines did not change the PSII activity in *T. elongatus* cells, the sensitivity to high light intensities of the mutant cells increased (Kirilovsky unpublished data). This E_m value of about

+200 mV opens the possibility that cyt *c*550 plays a role as an electron donor to the Mn_4Ca cluster in a photoprotective cycle involving a soluble redox component in the lumen [18]. The distance between the heme of the cyt *c*550 and the Mn_4Ca cluster is long (22 Å) meaning that the electron transfer will be in the ms-sec scale. This rate is slow relative to charge separation reactions but it remains potentially significant relative to charge recombination reactions (tens of seconds to min) occurring in PSII. This proposition must be demonstrated experimentally: it must be showed that cyt *c*550 is indeed capable to give electrons to the S_2 and S_3 states of the Mn_4Ca cluster and that it is reduced by a lumen component.

Acknowledgements

This work was supported by Grants: BFU2007-68107-C02-01 from the Spanish Ministry of Science and Innovation (MICINN) and PADI CVI-261 from the Andalusia Government**.** We would like to thank Dr. Anna Lindahl for critically reading the manuscript.

References

[1] A. Dolla, L. Blanchard, F. Guerlesquin, M. Bruschi, The protein moiety modulates the redox potential in cytochromes c, Biochimie 76 (1994) 471-479.

[2] P.D. Barker, S.J. Ferguson, Still a puzzle: why is haem covalently attached in c-type cytochromes?, Struct. Fold Des.7 (1999) 281-290.

[3] J.W.A. Allen, O. Daltrop, J.M. Stevens, S.J. Ferguson, C-type cytochromes: diverse structures and biogenesis systems pose evolutionary problems, Phil. Trans. R. Soc. Lond. B (2003) 358, 255–266.

[4] J.R. Shen, Y. Inoue, Cellular localization of cytochrome $c_{550.}$ Its specific association with cyanobacterial photosystem II, J. Biol. Chem. 272 (1993) 17821-17826.

[5] C.A. Kerfeld, D.W. Krogmann, Photosynthetic cytochromes c in cyanobacteria, algae and plants, Annu. Rev. Plant Physiol. Plant Mol. Biol. 49 (1998) 397–425.

[6] J.R. Shen, M. Qian, Y. Inoue, R.L. Burnap, Functional characterization of *Synechocystis* sp. 6803 ΔpsbU and ΔpsbV mutants reveals important roles of cytochrome c-550 in cyanobacterial oxygen evolution, Biochemistry 37 (1998) 1551-558.

[7] V. Fulop, J.W.B. Moir, S.J. Ferguson, J. Hajdu, The anatomy of a bifunctional enzyme: structural basis for reduction of oxygen to water and synthesis of nitric oxide by cytochrome cd_1, Cell 81 (1995) 369-377.

[8] C. Frazão, F.J. Enguta, R, Coelho, G.M. Sheldrick, J.A. Navarro, M. Hervás, M.A. De la Rosa, M.A. Carrondo, Crystal Structure of low-potential cytochrome c-549 from *Synechocystis* 6803 at 1.21 Å resolution, J. Biol. Inorg. Chem. 6 (2001) 324-332.

[9] J.M. Bowes, A.C. Stewart, D.S. Bendall, Purification of Photosystem II particles from *Phormidium laminosum* using the detergent dodecyl-β-d-maltoside. Properties of the purified complex, Biochim. Biophys. Acta 725 (1983) 210-219.

[10] C.W. Hoganson, G. Lagenfelt, L-E Andréasson, EPR and redox potentiometric studies of cytochrome c-549 of *Anacystis nidulans*, Biochim. Biophys. Acta 1016 (1990) 203-206.

[11] J.R. Shen, Y. Inoue, Binding and functional properties of two new extrinsic components, cytochrome c-550 and a 12-kDa protein in cyanobacterial photosystem II, Biochemistry 32 (1993) 1825-1832.

[12] J.R. Shen, R.L. Burnap, Y. Inoue, An independent role of cytochrome *c*-550 in cyanobacterial photosystem II as revealed by double-deletion mutagenesis of the *psbO* and *psbV* genes in *Synechocystis* sp. PCC 6803, Biochemistry 34 (1995) 12661-12668.

[13] R.W. Holton, J. Myers, Cytochromes of a blue-green algae: extraction of a c-type with a strongly negative redox potential, Science 142 (1963) 234-235.

[14] J. Alam, M.A. Sprinkle, M.A. Hermodson, D.W. Krogmann, Characterization of cytochrome c-550 from cyanobacteria, Biochim. Biophys. Acta 766 (1984) 317-321.

[15] J.A. Navarro, M. Hervás, B. De la Cerda, M.A. De la Rosa, Purification and physicochemical properties of the low potential cytochrome C549 from the cyanobacterium *Synechocystis* sp. PCC 6803, Arch. Biochem. Biophys. 3186 (1995) 46-52.

[16] M. Roncel, A. Boussac, J.L. Zurita, H. Bottin, M. Sugiura, D. Kirilovsky, J.M. Ortega, Redox properties of the photosystem II cytochromes *b*559 and *c*550 in the cyanobacterium *Thermosynechococcus elongatus*, J. Biol. Inorg. Chem. 8 (2003) 206-216.

[17] J.S. Vrettos, M.J. Reifler, O. Kievit, K.V. Lakshmi, J.C. de Paula, G.W. Brudvig, Factors that determine the unusually low reduction potential of cytochrome c550 in cyanobacterial photosystem II, J. Biol. Inorg. Chem. 6 (2001) 708-716.

[18] F. Guerrero, A. Sedoud, D. Kirilovsky, A.W. Rutherford, J.M Ortega, M. Roncel, A high redox potential form of cytochrome c_{550} in photosystem II from *Thermosynechococcus elongatus,* J. Biol. Chem. 286 (2011) 5985–5994.

[19] A. Guskov, J. Kern, A. Gabdulkhakov, M. Broser, A. Zouni, W. Saenger, Cyanobacterial photosystem II at 2.9-Å resolution and the role of quinones, lipids, channels and chloride, Nature Struct. Biol. 16 (2009) 334–342.

[20] C.C. Moser, C.C. Page, P.L. Dutton, Tunneling in PSII, Photochem. Phobiol. Sci. 4 (2005) 933-939.

[21] D.W. Krogmann, S. Smith, Low potential cytochrome *c*550 function in cyanobacteria and algae, in: M Baltscheffsky (Ed.), Current Research in Photosynthesis, Vol II**.** Kluwer Academic, Dordrecht, The Netherlands, 1990, pp 687-690.

[22] D.W. Krogmann, The low-potential cytochrome c of cyanobacteria and algae, Biochim. Biophys. Acta 1058 (1991) 35-37.

[23] K.K. Ho, C.A. Kerfeld, D.W. Krogmann, The water-soluble cytochromes of cyanobacteria, in: G.A. Peschek, C. Obinger, G. Renger (Eds.), Bioenergetic processes of cyanobacteria: from evolutionary singularity to ecological diversity, Springer, Dordrecht, 2011, pp. 515-540.

[24] K.N. Ferreira, T.M. Iverson, K. Maghlaoui, J. Barber, S. Iwata, Architecture of the photosynthetic oxygen evolving center, Science 303 (2004) 1831–1838.

[25] J. Biesiadka, B. Loll, J. Kern, K.D. Irrgang, A. Zouni, Crystal structure of cyanobacterial photosystem II at 3.2 Å resolution: a closer look at the Mn-cluster. Phys. Chem. Chem. Phys. 6 (2004) 4733–4736.

[26] A. Zouni, H.T. Witt, J. Kern, P. Fromme, N. Krauβ, W. Saenger, P. Orth, Crystal Structure of oxygen evolving Photosystem II from *Synechococcus elongatus* a 3.8 Å resolution, Nature 409 (2001) 739-743.

[27] Y. Umena, K. Kawakami, J-R. Shen, N. Kamiya, From crystal structure of oxygen-evolving photosystem II at a resolution of 1.9 Å, Nature 473 (2011) 55–60.

[28] J.L. Roose, K.M. Wegener, H.B. Pakrasi, The extrinsic proteins of Photosystem II, Photosynth. Res. 92 (2007) 369-387.

[29] L.E. Thornton, J.L. Roose, H.B. Pakrasi, M. Ikeuchi, The low molecular weight proteins of photosystem II in: T.J. Wydrynski, K. Satoh (Eds.), Photosystem II: The light-driven water-plastoquinone oxidoreductase. Advances in photosynthesis and respiration, Vol 22, Springer, Dordrecht, 2005, pp. 121-137.

[30] H. Ohta, T. Suzuki, M. Ueno, A. Okumura, S. Yoshihara, J-R Shen, I. Enami, Extrinsic proteins of photosystem II. An intermediate member of the PsbQ protein family in red algal PS II, Eur. J. Biochem. 270 (2003) 4156–4163.

[31] M. Krinner, G. Hauska, E. C. Hurt, W. Lockau, A cytochrome b6f complex with plastoquinol/plastocyanin reductase activity from *Anabaena variabilis*, Biochim. Biophys. Acta 681 (1982) 110-117.

[32] C.W. Hoganson, P.A. Casey, O. Hansson, Flash photolysis studies of manganese-depleted Photosystem II: evidence for binding of the Mn^{2+} and other transition metal ions, Biochim. Biophys. Acta 1057 (1991) 399-406.

[33] J.R. Shen, M. Ikeuchi, Y. Inoue, Stoichiometric association of extrinsic cytochrome c550 and 12 kDa protein with a highly purified oxygen-evolving photosystem II core complex from Synechococcus vulcanus, FEBS Lett. 301 (1992) 145-149.

[34] N. Kamiya, J.-R. Shen, Crystal structure of oxygen-evolving photosystem II from *Thermosynechococcus vulcanus* at 3.7-Å resolution, Proc. Natl. Acad. Sci. USA 100 (2003) 98–103.

[35] I. Enami, H. Murayama, H. Ohta, M. Kamo, K. Nakazato, J.-R. Shen, Isolation and characterization of a Photosystem II complex from the red alga *Cyanidium caldarium:* association of cytochrome c-550 and a 12 kDa protein with the complex, Biochim. Biophys. Acta 1232 (1995) 208-216.

[36] P.K. Evans, D.W. Krogmann, Three c-type cytochromes from the red alga *Porphyridium cruentum*, Arch. Biochem. Biophys. 227 (1983) 494-510.

[37] M. Reith, J. Mulholland, A high-resolution gene map of the chloroplast genome of the red alga *Porphyra purpurea*, Plant Cell 5 (1993) 465-475.

[38] T. Yamanaka, H. De Klerk, M.D. Kamen, Highly purified cytochromes c derived from the diatom *Navicula pelliculosa*, Biochim. Biophys. Acta 143 (1967) 426-424.

[39] K. Shimazaki, K. Takamiya, M. Nishimura, Studies on electron transfer systems in the marine diatom *Phaeodactylum tricornutum.* I. Isolation and characterization of cytochromes, J. Biochem. 83 (1978) 1631-1638.

[40] K. Kowallik, B. Stroebe, I. Schaffran, U. Freier, The chloroplast genome of a chlorophyll a+c containing alga, *Odontella sinensis*. Plant Mol Biol. Rep 13 (1995) 336–342.

[41] I. Enami, S. Yoshihara, A. Tohri, A. Okumura, H. Ohta, J.-R. Shen, Cross-reconstitution of various extrinsic proteins and photosystem II complexes from cyanobacteria, red algae and higher plants, Plant Cell Physiol. 41 (2000) 1354–1364.

[42] I. Enami, M. Iwai, A. Akiyama, T. Suzuki, A. Okumura, T. Katoh, O. Tada, H. Ohta, J.-R. Shen, Comparison of binding and functional properties of two extrinsic components, cyt *c*550 and a 12 kDa protein, in cyanobacterial PSII with those in red algal PSII, Plant Cell Physiol. 44 (2003) 820–827.

[43] G. Glöckner, A. Rosenthal, K. Valentin, The structure and gene repertoire of an ancient red algal plastid genome, J. Mol. Evol. 51 (2000) 382-390.

[44] V.L. Stirewalt, C.B. Michalowski, W. Loffelhardt, H.J. Bohnert, D. Bryant, Nucleotide sequence of the cyanelle genome from *Cyanophora paradoxa*, Plant Mol. Biol. 13 (1995) 327–332.

[45] Y. Kamimura, T. Yamasaki, E. Matsuzaki, Cytochrome components of green alga, *Bryopsis maxima*, Plant Cell Physiol. 18 (1977) 317-324.

[46] K. Tamura, J. Dudley, M. Nei, S. Kumar (2007) MEGA4: Molecular Evolutionary Genetics Analysis (MEGA) software version 4.0. Molecular Biology and Evolution 10.1093/molbev/msm092.

[47] S.B. Gould, R.F. Waller, G.F. McFadden, Plastid evolution. Annu. Rev. Plant. Biol. 59 (2008) 491-517.

[48] E.C. Nowack, M. Melkonian, G. Glockner, Chromatophore genome sequence of Paulinella sheds light on acquisition of photosynthesis by eukaryotes, Curr. Biol. 18 (2008) 410-418.

[49] H. Katoh, S. Itoh, J.-R. Shen, M. Ikeuchi, Functional analysis of *psb*V and a novel c-type cytochrome gene *psb*V2 of the thermophilic cyanobacterium Thermosynechococcus elongatus strain BP-1, Plant Cell Physiol. 42 (2001) 599–607.

[50] C.A. Kerfeld, M.R. Sawaya, H. Bottin, K.T. Tran, M. Sugiura, D. Cascio, A. Desbois, T.O. Yeates, D. Kirilovsky, A. Boussac, Structural and EPR characterization of the soluble form of cytochrome c-550 and of the *psbV2* gene product from cyanobacterium *Thermosynechococcus elongatus*, Plant Cell Physiol. 44 (2003) 697–706.

[51] H. Andrews, Z. Li, A. Altuve-Blanco, M. Rivera, R.L. Burnap, Expression, mutagenesis, and characterization of recombinant low-potential cytochrome *c*550 of Photosystem II, Biochemistry 44 (2005) 6092-6100.

[52] D. Kirilovsky, M. Roncel, A. Boussac, A. Wilson, J.L. Zurita, J.M. Ducruet, H. Bottin, M. Sugiura, J.M. Ortega, A.W. Rutherford, Cytochrome *c*550 in the cyanobacterium *Thermosynechococcus elongatus*: study of redox mutants. J. Biol. Chem. 279 (2004) 52869–52880.

[53] R.W. Holton, J. Myers, Water-soluble cytochromes from a blue-green alga. I. Extraction, purification, and special properties of cytochromes c (549, 552, and 554 *Anacystis nidulans*), Biochim. Biophys. Acta 131 (1967) 362-374.

[54] R.W. Holton, J. Myers, Water-soluble cytochromes from a blue-green alga. II. Physicochemical properties and quantitative relationships of cytochromes c (549, 552, and 554 *Anacystis nidulans*), Biochim. Biophys. Acta 131 (1967) 375-384.

[55] M.R. Sawaya, D.W. Krogmann, A. Serag, K.K. Ho, T.O. Yeates, C.A. Kerfeld, Structures of cytochrome c-549 and cytochrome c6 from the cyanobacterium *Arthrospira maxima*, Biochemistry 40 (2001) 9215-9225.

[56] J. Peisach, W.E. Blumberg, A. Adler, Electron paramagnetic resonance studies of iron porphyrin and chlorine systems, Ann. N.Y. Acad. Sci. 206 (1973) 310-327.

[57] F.A. Walker, Magnetic spectroscopic (EPR, ESEEM, Mossbauer, MCD and NMR) studies of low-spin ferriheme centers and their corresponding heme proteins, Coord. Chem. Rev. 186 (1999) 471-534.

[58] D. Lefevre-Groboillot, S. Dijols, J.-L. Boucher, J.-P. Mahy, R. Ricoux, A. Desbois, J.-L. Zimmermann, D. Mansuy, N-hydroxyguanidines as new heme ligands: UV-visible, EPR, and resonance Raman studies of the interaction of various compounds bearing a C=NOH function with microperoxidase-8, Biochemistry 40 (2001) 9909–9917.

[59] R. Quin, J.S. Valentine, M.P. Byrn, C.E. Strouse, Electronic structure of low-spin ferric porphyrins : A single-crystal EPR and structural investigation of the influence of axial ligands orientation and the effects of pseudo-Jahn-Teller distortion, J. Am. Chem. Soc. 109 (1987) 3301-3308.

[60] T.C. Strekas, T.G. Spiro, Cytochrome c: resonance Raman spectra, Biochim. Biophys. Acta 278 (1972) 188-192.

[61] M. Friedman, D.L. Rousseau, F. Adar, Excited state lifetimes in cytochromes measured from Raman scattering data: evidence for iron-porphyrin interactions. Proc. Natl. Acad. Sci. USA 74 (1977) 2607-2611.

[62] S. Hu, I.K. Morris, J.P. Singh, K.M. Smith, T.G. Spiro, Complete assignment of cytochrome c resonance Raman spectra via enzymatic reconstitution with isotopically labeled hemes. J. Am. Chem. Soc. 115 (1993) 12446–12458.

[63] T.G. Spiro, Resonance Raman spectroscopy as a probe of heme protein structure and dynamics. Adv. Prot. Chem. 37 (1985) 111-159.

[64] A. Desbois, Resonance Raman spectroscopy of c-type cytochromes. Biochimie 76 (1994) 693–707.

[65] T.G. Spiro, Resonance Raman spectra of heme and metalloproteins. Biological applications of Raman spectroscopy, Vol 3, Wiley, New York, 1988.

[66] M. Abe, T. Kitagawa, Y. Kyogoku, Resonance raman spectra of octaethylporphyrinato-Ni (II) and meso-deuterated and 15N substituted derivatives. II. A normal coordinate analysis, J. Chem. Phys. 69 (1978) 4526-4534.

[67] D.M. Collins, R. Countryman, J.L. Hoard, Stereochemistry of low-spin iron porphyrins. I. Bis(imidazole)-alpha,beta,gamma,delta-tetraphenylporphinatoiron(3) chloride, J. Am. Chem. Soc. 94 (1972) 2066-2072.

[68] T. Kitagawa, Y. Kyogoku, T. Iizuka, M. Ikeda-Saito, T. Yamanaka, Resonance Raman scattering from hemoproteins, Effects of ligands upon the Raman spectra of various c-type cytochromes. J. Biochem. 78 (1975) 719–728.

[69] A. Krieger, A.W. Rutherford, G.N. Johnson, On the determination of redox midpoint potential of the primary quinone electron acceptor, QA, in Photosystem II, Biochim. Biophys. Acta 1229 (1995) 193-201.

[70] G.R. Moore and G.W. Pettigrew, Cytochromes c: evolutionary, structural and physicochemical aspects, Springer, Berlin, 1990.

[71] P. Bertrand, O. Mbarki, M. Asso, L. Blanchard, F. Guerlesquin, M. Tegoni, Control of the redox potential in c-type cytochromes: importance of the entropic contribution, Biochemistry, 34 (1995) 11071–11079.

[72] F.A. Tezcan, J.R. Winkler, H.B. Gray, Effects of ligation and folding on reduction potentials of heme proteins, J. Am. Chem. Soc. 120 (1998) 13383–13388.

[73] B. Dalhus, M. Saarinen, U.H. Sauer, P. Eklund, K. Johansson, A. Karlsson, S. Ramaswamy, A. Bjørk, B. Synstad, K. Naterstad, R. Sirevåg, H. Eklund**,** Structural basis for thermophilic protein stability: structures of thermophilic and mesophilic malate dehydrogenases, J. Mol. Biol. 318 (2002) 707-21.

[74] B. Loll, J. Kern, W. Saenger, A. Zouni, J. Biesiadka, Towards complete cofactor arrangement in the 3.0 A resolution structure of photosystem II, Nature 438 (2005) 1040-1044.

[75] B. Loll, Photosystem II from the Cyanobacterium *Thermosynechococcus elongatus* at 3.2-Å Resolution, Ph.D. Thesis, 2005, Freie Universität Berlin, Berlin, Germany

[76] M. Beissinger, H. Sticht, M. Sutter, A. Ejchart, W. Haehnel, P. Rösch, Solution structure of cytochrome c6 from the thermophilic cyanobaterium Synechococcus elongates, EMBO J. 17 (1998) 27-36.

[77] F. Sommer, F. Drepper, W. Haehnel, M. Hippler, Identification of precise electrostatic recognition sites between cytochrome c6 and the photosystem I ububit PsaF using mass spectrometry, J. Biol. Chem. 281 (2006) 35097-35103.

[78] F. Guerrero, Citocromos asociados al Fotosistema II en la cianobacteria termófila *Thermosynechococcus elongatus*. Estudio de mutantes puntuales del citocromo *b*559 y análisis redox del citocromo *c*550, Ph.D. Thesis, 2011, Universidad de Sevilla, Sevilla, Spain.

[79] L. Wang, A.B. Cowley, S. Terzyan, X. Zhang, D.R. Benson, Comparison of cytochromes b5 from insects and vertebrales, Proteins 67 (2007) 293-304.

[80] G.V. Louie, G.D. Brayer, High-resolution refinement of yeast iso-1-cytochrome c and comparisons with other eukaryotic cytochromes c, J. Mol. Biol. 214 (1990) 527-555.

[81] H.L. Axelrod, G. Feher, J. P. Allen, A.J. Chirino, M.W. Day, B.T. Hsu, D.C. Rees Crystallization and X-ray structure determination of cytochrome c2 from Rhodobacter sphaeroides in three crystal forms. Acta Crystallogr. D Biol. Crystallogr. 50 (1994) 596-602.

[82] S. Sogabe and K. Miki, Refined crystal structure of ferrocytochrome c2 from Rhodopseudomonas viridis at 1.6 A resolution, J. Mol. Biol. 252 (1995) 235-47.

[83] Y. Matsuura, T. Takano and R.E. Dickerson, Structure of cytochrome c551 from *Pseudomonas aeruginosa* refined at 1.6 Å resolution and comparison of the two redox forms, J. Mol. Biol. 156 (1982) 389–409.

[84] L.Z. Morand, R.H. Cheng, D.W. Krogmann in: Bryant DA (Ed.) The Molecular Biology of Cyanobacteria, Kluwer Academic Publishers, Dordrecht, 1994, pp 381-407.

[85] C. Kang, R.P. Chitnis, S. Smith, D.W. Krogmann, Cloning and sequence analysis of the gene encoding the low potential cytochrome c of *Synechocystis* PCC 6803, FEBS Lett. 344 (1994) 5-9.

[86] P.F. Kinzel, G.A. Pescheck, Oxidation of *c*-type cytochromes by the membrane-bound cytochrome oxidase (cytochrome aa_3) of blue-green algae, Plant Physiol. 69 (1982) 580-584.

[87] Y. Nishiyama, H. Hayashi, T. Watanabe, N. Murata, Photosynthetic oxygen evolution is stabilized by cytochrome *c550* against heat inactivation in *Synechococcus* sp. PCC 7002**,** Plant Physiol. 105 (1994) 1313-1319.

Figure legends

Figure1. Phylogenetic tree of the evolutionary relationships between cytochromes *c*550 of cyanobacteria and photosynthetic eukaryotes.

Phylogenetic analyses were conducted in MEGA4 program using the Minimum Evolution method [46]. The bootstrap consensus tree was inferred from 1000 replicates. The evolutionary distances are in the units of number of amino acid substitutions per site. Accession numbers of annotated and non-annotated sequences identified in databases are shown after the corresponding species names. Oval: the phototrophic amoeba *Paulinella chormatophora*. Boxed: two sequences of dinotoms (Dinophyta having endosymbiotic diatoms).

Figure 2. Difference absorption spectra of the cytochromes bound to the photosystem II reaction center in *T. elongatus.*

Redox difference absorption spectra of cytochromes *b*559 and *c*550 in PSII core complexes from *T. elongatus* at pH 6.5 were obtained during the course of a redox titration by subtracting absolute spectra recorded at –300 mV minus +458 mV (spectrum 1) and at –300 mV minus +55 mV (spectrum 2). Redox titration procedure and sample composition are described [16, 18]. Solid and dotted vertical lines indicate 559 and 550 nm wavelengths, respectively.

Figure 3. Reductive potentiometric titrations of cytochrome *c*550 in its purified state and bound to PSII

Plots of the percentages of reduced cyt *c*550 obtained from the absorbance differences at 550-538 nm *versus* ambient redox potentials in its purified state (A) and bond to PSII in the presence (B) and in the absence of redox mediators (C). Redox titrations were carried out at

pH 6.0 as described in [16, 18]. The *solid curves* represent the best fits of the experimental data to the Nernst equation in accordance with one-electron processes (n=1) for one component.

Figure 4. Partial representation of the three dimensional structure of cytochrome *c*550 in its soluble form (A) and in its native state bound to PSII (B). Fifteen of the completely conserved residues of cyt c550 are shown (Thr9, Lys47, Leu54, Leu59, Ala62, Pro64, Pro79, Tyr82, Asp83, Gly84, Pro93, Arg105, Trp130, Gly131, Gly132). N and C indicate the amino- and carboxy-terminus of the cyt *c*550. The heme and the coordinating histidines are shown as sticks. All other subunits are shown as "cartoon" in different colours. OEC is shown as spheres. Figures have been made using PyMol and the PDB files 3BZ2 and 1MZ4.

Table 1

Table 1. List of selected organisms containing *psb*V gen from GenBank Database (http://www.ncbi.nlm.nih.gov) (27th October 2011)

CYANOBACTERIA		EUKARYOTA	
Section I	*Thermosynechococcus elongatus BP-1*	**Glaucocystophyta**	*Cyanophora paradoxa*
	Synechococcus elongatus PCC 6301	**Rhodophyta or Red algae**	*Gracilaria tenuistipitata var. Liui*
	Microcystis aeruginosa NIES-843		*Cyanidioschyzon merolae 10D*
	Cyanothece sp. PCC 7425		*Cyanidium caldarium*
	Synechocystis sp. PCC 6803		*Porphyra yezoensis*
	Acaryochloris marina MBIC11017		*Porphyra purpurea*
	Aphanothece halophytica	**Stramenopiles**	
	Prochlorococcus marinus str. MIT 9303	Diatoms	*Fistulifera sp. JPCC DA0580*
	Gloeobacter violaceus PCC 7421		*Thalassiosira pseudonana*
	Cyanobium PCC 7001		*Thalassiosira oceanica*
	Aphanizomenon flos-aquae		*Phaeodactylum tricornutum*
	Cylindrospermopsis raciborskii CS-505		*Odontella sinensis*
	Crocosphaera watsonii WH501	Pelagophyceae	*Aureococcus anophagefferens*
	Nodularia spumigena CCY9414		*Aureoumbra lagunensis*
	Raphidiopsis brookii D9	Phaeophyceae	*Ectocarpus siliculosus*
	Mycrocoleus vaginatus FGP-2		*Fucus vesiculosus*
		Raphidophyceae	*Heterosigma akashiwo*
		Xanthophyceae	*Vaucheria litorea*
Section III	*Trichodesmium erythraeum IMS101*	**Haptophyta**	*Emiliania huxleyi*
	Arthrospira maximaCS-328	**Alveolata**	
	Lyngbya PCC 8106	Chromerida	*Chromera velia*
			Chromerida sp. RM11
		Dinophyceae	*Durinskia baltica*
Section IV	*Nostoc sp. PCC 7120*		*Kryptoperidinium foliaceum*
	Nostoc punctiforme PCC 73102		*Karlodinium veneficum*
	Anabaena variabilis ATCC 29413	**Cryptophyta**	*Rhodomonas salina*
	Oscillatoria PCC 6506		*Guillardia theta*
		Rhizaria	*Paulinella chromatophora*

Table 2

Table 2. Summary of midpoint redox potentials of cytochrome *c*550

Cyanobacteria	E_m	**Ref.**
Soluble form		
*Spirulina máxima**	-260 mV	[54]
Synechococcus sp. *PCC 6301***	-280 mV	[10]
Synechocystis sp. *PCC 6803*	-250 mV	[15]
Thermosynechoccocus elongatus	-240 mV	[16]
Synechocystis sp. PCC 6803 (adsorbed to an electrode)	-108 mV	[17]
Bound form		
Thermosynechoccocus elongatus (with 14 redox mediators)	-80 mV	[16]
Thermosynechoccocus elongatus (with 8 redox mediators)	-20 mV	[18]
Thermosynechoccocus elongatus (with DAD)	+215 mV	[18]
Thermosynechoccocus elongatus (without redox mediators)	+200 mV	[18]

**Arthrospira maxima; ** Anacystis nidulans*

Table 3

Table 3. Cytochrome *c*550 Primary Structure Alignment

```
                          10        20        30        40        50        60        70
T. elongatus          AELTPEVLTV PLNSEGKTIT LTEKQYLEGK RLFQYACASC HVGGITKTNP SLDLRTETLA LATPPRDNIE
Synechococcus         AELTAETRTV KLNPQGDNVT LSLKQVAEGK QLFAYACGQC HVGGITKTDP NVGLDPEALA LATPPRDSVE
Nostoc                LELDEATRTV PLNAQGDTVT LSLKQVKEGK RLFQYACAQC HVGGVTKTNQ NVGLEPEALA LATPNRNNIE
A. variabilis         LELDEATRTV PLNAQGDTVT LSLKQVKEGK RLFQYACAQC HVGGVTKTNQ NVGLEPEALA LATPNRNNIE
P. marinus            AQWDAETLTV PAGSGGQQVT FSESEIKSAS KLFKSNCATC HNQGVTKTNQ NVGLDLEALS LASPARDNVD
A. marina             AELDDATRTV ALNEG-STVT LSTQQAKEGQ RLFNFACANC HIGGDTKTNP SINLSSASLA GANPRRDNVE
A. maxima             LELTEELRTL PINAQGDTAV LSLKEIKKGQ QVFNAACAQC HALGVTKTNP DVNLSPEALA LATPPRDNIA
M. aeruginosa         LELNEKTLTI TLNDAGESVT LTSEQATEGQ KLFVANCTKC HLQGKTKTNN NVSLGLGDLA KAEPPRDNLL
Synechocystis         VELTESTRTI PLDEAGGTTT LTARQFTNGQ KIFVDTCTQC HLQGKTKTNN NVSLGLADLA GAEPRRDNVL
C. paradoxa           AALDEETRTV ALNST-ETVV LTPEQVKRGK RLFNSTCGIC HVGGITKTNP NVGLDSEALA LATPPRNNIE
C. caldarium          LELNEEARTV KLNSEGQSLT LNEEQIKKGK RLFNSHCGSC HVGGITKTNP NVGLDLESLN GANPPRNNIN
Porphyra              IELDEATRTV PLESSGRTVV LTPEQVKRGK RLFNNSCAIC HNGGITKTNP NVGLDPESLG LATPQRDNIE
Gracilaria            MELDEATRTV TLEESGKTIT LTPEQVKRGK RLFNNSCAQC HNGGITKTNP NIGLDPESLS GATPVRDNIR
Fistulifera           IELDEATRTV VADGSGKTIV LTPEQVKRGK RLFNATCGAC HVGGITKTNP NVGLDPEALS LATPRRDNIA
P. tricornutum        IDLDEATRTV VVDSSGKTIV LTPEQVKRGK RLFNATCGAC HVGGVTKTNP NVGLDPEALS LATPRRDNIA
T. pseudonana         IDLDEATRTV VTDSSGNTTV LTPEQVKRGK RLFNATCGAC HTGGITKTNP NVGLDPEALS LATPRRDNIS
O. sinensis           IDLDEATRTV VADSNGNTTV LTPEQVKRGK RLFNNTCGAC HVGGVTKTNP NVGLRPEGLS LATPRRDNAA
F. vesiculosus        IELDEATRTI PVTSDGKTTI LTPEQVKRGK RLFNSSCGQC HVGGVTKTNP NLGLDPEALS LATPARNNIN
Chromera              RSLTDSIRTV KLSENNDKAI ITPNELGRGK VLFAKTCSAC HTGGITKTNP NIGLALSTLK NAIPERDNVV
Durinskia             IDLDEATRTV VKDASGKTVV LTPEQVKRGK RLFNATCGAC HVGGITKTNP NVGLDPEALS LATPRRDNID
Karlodinium           LDLKENIRTV SFDTTDKIVV ITKTQIKRGK RLFTNACANC HVGGVTKPDP NIGLDMIALR FATPPKNNIV
                             *:        :.  :   ..  :*   *  * *  * **.:  .:.*    *   * * ::.
```

```
                                  80          90          100         110         120         130
T. elongatus                GLVDYMKNPT TYDGEQEIAE VHPSLRSADI FPKMRNLTEK DLVAIAGHIL VEPKILGDKW GGGKVYY
Synechococcus               SLVDYLHNPT TYDGEREISE LHPSTKSTDI FPKMRNLTED DLVAISGHIL LQPKIVGTKW GGGKIYY
Nostoc                      GLVDYMKNPT TYDGVEEISE IHPSLKSADI FTAMRNLTDK DLESIAGHIL LQPKILGDKW GGGKIYY
A. variabilis               GLVDYMKNPT TYDGVEEISE IHPSIKSADI FTAMRNLTDK DLESIAGHIL LQPKILGDKW GGGKIYY
P. marinus                  GLVEFLKNPM SYDGEYSIAD THPGISSSDV YVQMRTLNDE DLRLIAGYIL TAEKVQGDQW GGGKIYF
A. marina                   GLVDYMNNPT TYDGFDTISE VHPSTQSTDV FPLMRNLSDE DLFDIAGHIL IQPSVIGDQW GGGKANR
A. maxima                   ALVDYVKNPT TYDGFIEIYE LHPSLKSADI FPKMRNLSED DLYNVAAYIL LQPKVRGEQW GGGKYLR
M. aeruginosa               ALIDYLEHPT SYDGEDDLSE LHPNVSRPDI FPELRNLTED DVYNVAAYML VAPRL-DERW GG-TIYF
Synechocystis               ALVEFLKNPK SYDGEDDYSE LHPNISRPDI YPEMRNYTED DIFDVAGYTL IAPKL-DERW GG-TIYF
C. paradoxa                 SLVDYMKNPT SYDGSEEIYD IHPSIRSADA FPKMRNLTEE DLYDIAGHIL LSPKILPSQW GGGKIYY
C. caldarium                ALVEYMKDPK TYDGSESIAE IHPSIKSADI FPKMRDLSDD DLKVIAGHIL VQPKINSEKW GGGKIYY
Porphyra                    ALVDYMKDPT SYDGAESIAE LHPSIKSAEI FPKMRNLTDE DLFTIAGHIL LQPKIVSEKW GGGKIYY
Gracilaria                  NLIEYIKDPT SYDGATSIAE LHPSIKSAEI FPKMRNLTDE DLFAIAGHIL IQPKIAAEKW GGGKIYY
Fistulifera                 SLVDYMKNPT TYDGLESIAE VHPSIKSADI YPRMRSVTEE DLTAMAGHIL LSPKVLSEKW GGGKIYY
P. tricornutum              GLVDFLKNPT TYDGLESIAE VHPSIKSADI YPRMRSVTDE DLTAMAGHIL LQPKIVTEKW GGGKIYY
T. pseudonana               ALVDYLKNPT TYDGLESIAE IHPSIKSADI YPRMRSLTDE DLYSIAGHIM LQPKIVAEKW GGGKIYF
O. sinensis                 ALVDYLKNPT SYDGLESIAE IHPSIKSGDI YPRMRSLTDE DLFSIAGHIL LQPKIVTEKW GGGKIYY
F. vesiculosus              ALVDYMKNPT TYDGLESIAE IHPSIKSANI FTRMRSLDEK DLVDIAGHIL LQPKIVSEKW GGGKIYY
Chromera                    NLVQYMKYPT AYDGTFTLNE THPNTTFAVF FPSMRTLTEK DLYSIAGYIL VQAQVLGEKW GGGKVYY
Durinskia                   ALIDYLKNPT SYDGLDSIAE VHPSIKSADL YPRMRSVTDD DLYAMAGHIL LQPKIVTEKW GGGKIYY
Karlodinium                 NLVAYFKDPI TYDGLYSISE LHPSIKGADL FPKMRFLTDE DLFSVAGYIL YQYNILGDRW GGGKVYY
                             *: :.. *  :***     :  **.       :  :*   :. *:  ::.: :     :   :* ** .
```

Complete names of the organisms included in the table are: *T. elongatus, Thermosynechococcus elongatus* (gi_58177112); *Synechococcus, Synechococcus* sp. *PCC 6301* (BAD80275); *Nostoc, Nostoc sp.* PCC 7120 (BAB77783); *A. variabilis, Anabaena variabilis* (ABA22359); *P. marinus, Prochlorococcus marinus* (YP_001016548); *Acaryochoris marina, A. marina* (YP_001518187); *A. maxima, Arthrospira maxima* (ZP_03274665); *M. aeruginosa, Microcystis aeruginosa* (YP_001656196); *Synechocystis, Synechocystis* sp. *PCC 6803* (BAA18512); *C. paradoxa, Cyanophora paradoxa* (NP_043260); *C. caldarium, Cyanidium caldarium* (NP_045156)*; Porphyra, Porphyra purpurea* (AAC08085); *Gracilaria, Gracilaria tenuistipitata var. liui* (YP_063518); *Fistulifera, Fistulifera* sp. *JPCC DA0580* (YP_004376577); *P. tricornutum, Phaeodactylum tricornutum* (YP_874401); *T. pseudonana, Thalassiosira pseudonana* (YP_87449); *O. sinensis, Odontella sinensis* (NP_043700); *F. vesiculosus, Fucus vesiculosus* (CAX12410); *Chromera, Chromera velia* (ADJ66524); *Durinskia, Durinskia baltica* (YP_003734993); *Karlodinium, Karlodinium veneficum* (AEJ72991).

KEY (each species name is followed by its data base Accession Numbers in parentheses). Conserved Cys and His residues are in black bold and red bold, respectively. Identical, strongly and weakly similar residues were indicated by (*), (:) and (.), respectively.

Table 4

Table 4. Summary of functions proposed for cytochrome *c*550

Form	Function	Ref.
Soluble form		
	Anaerobic disposal of electron from carbohydrate reserves	[21]
	Anaerobic fermentation	[21, 22]
	Removing excess electrons in anaerobic grown cells	[86]
	Hydrogenase reactions	[54]
	Nitrate reduction	[14]
	Endogenous cofactor for cyclic phosphorylation	[11]
	Detoxifying reactive oxygen species	[51]
Bound form		
	Enhacing O_2 evolution by facilitating the binding of another extrinsic proteins (12 kD)	[11, 33]
	Acting as a barrier to reductive attack on the Mn_4Ca cluster	[52]
	Electron acceptor to remove excess electron under conditions where photosynthesis is not maximal	[28]
	Electron donor to the Mn_4Ca cluster in a protective cycle	[18]

Figure 1

Fig. 1

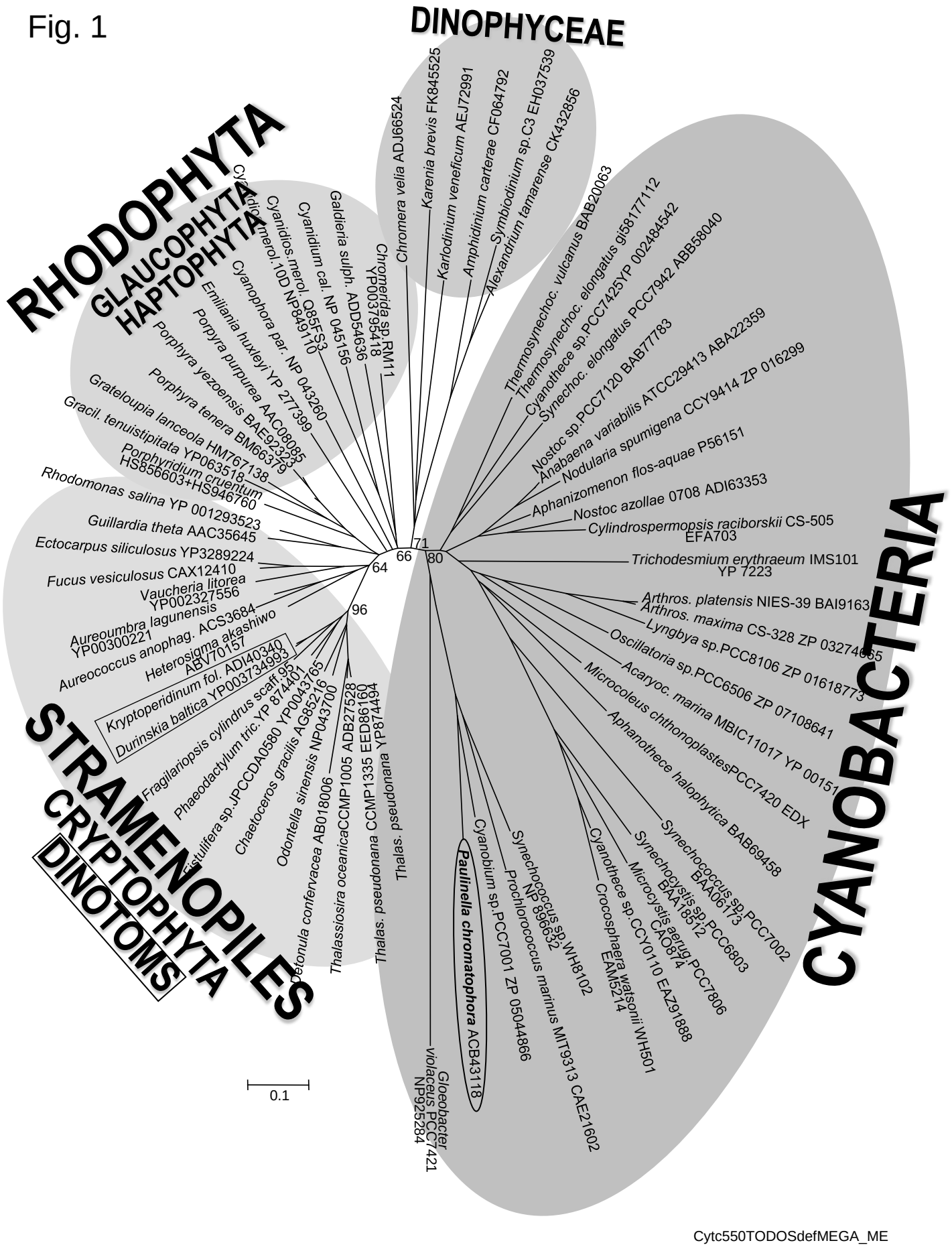

Figure 2

Fig. 2

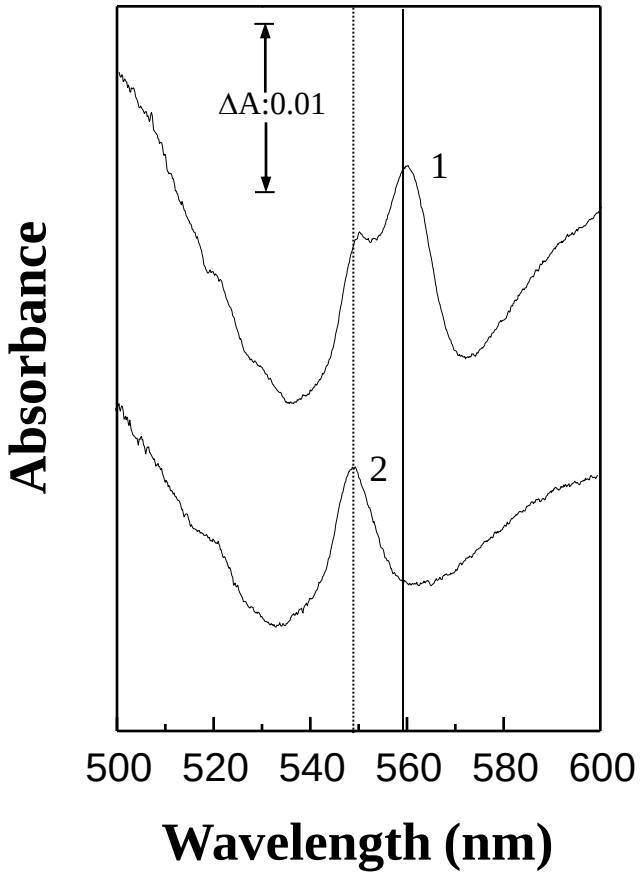

Figure 3

Fig. 3

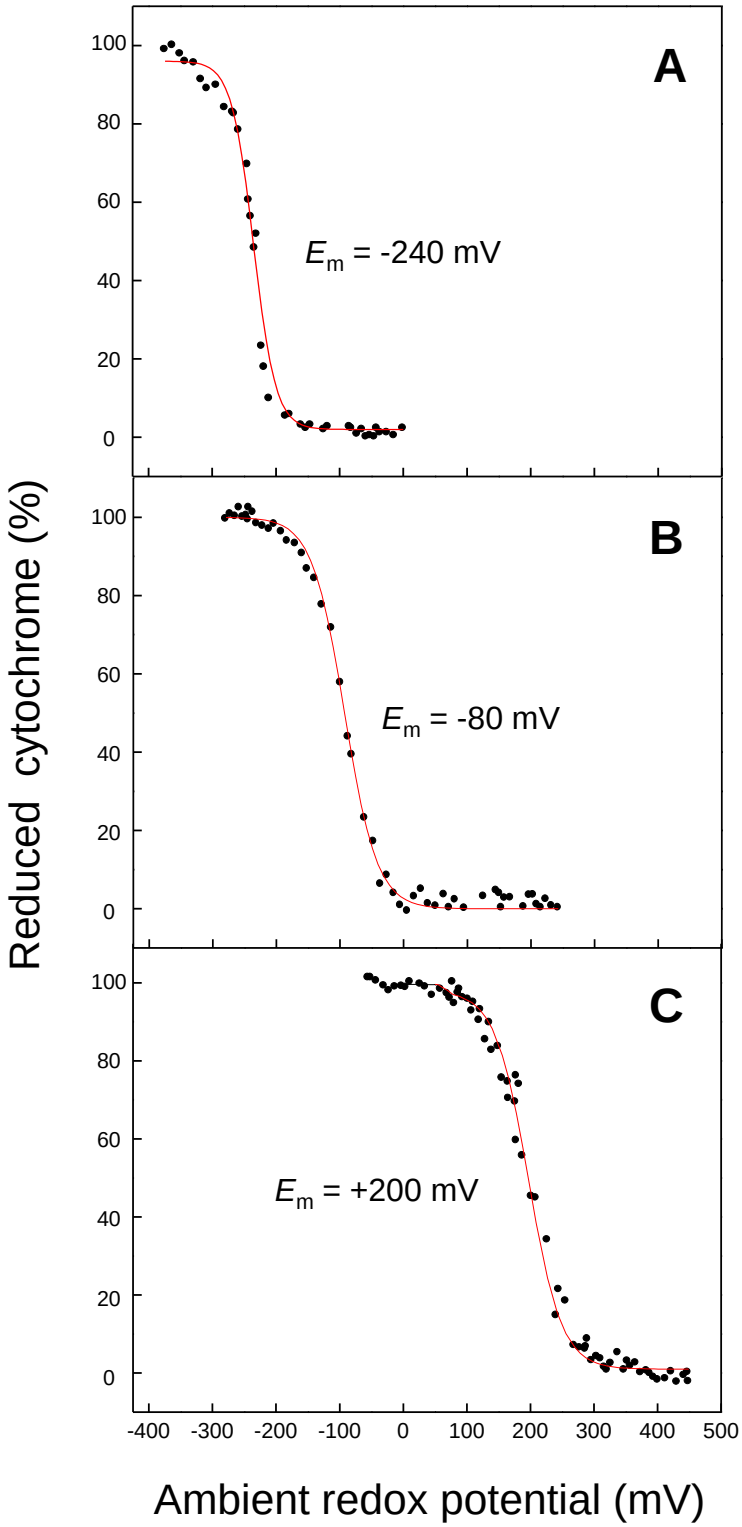

Figure 4A

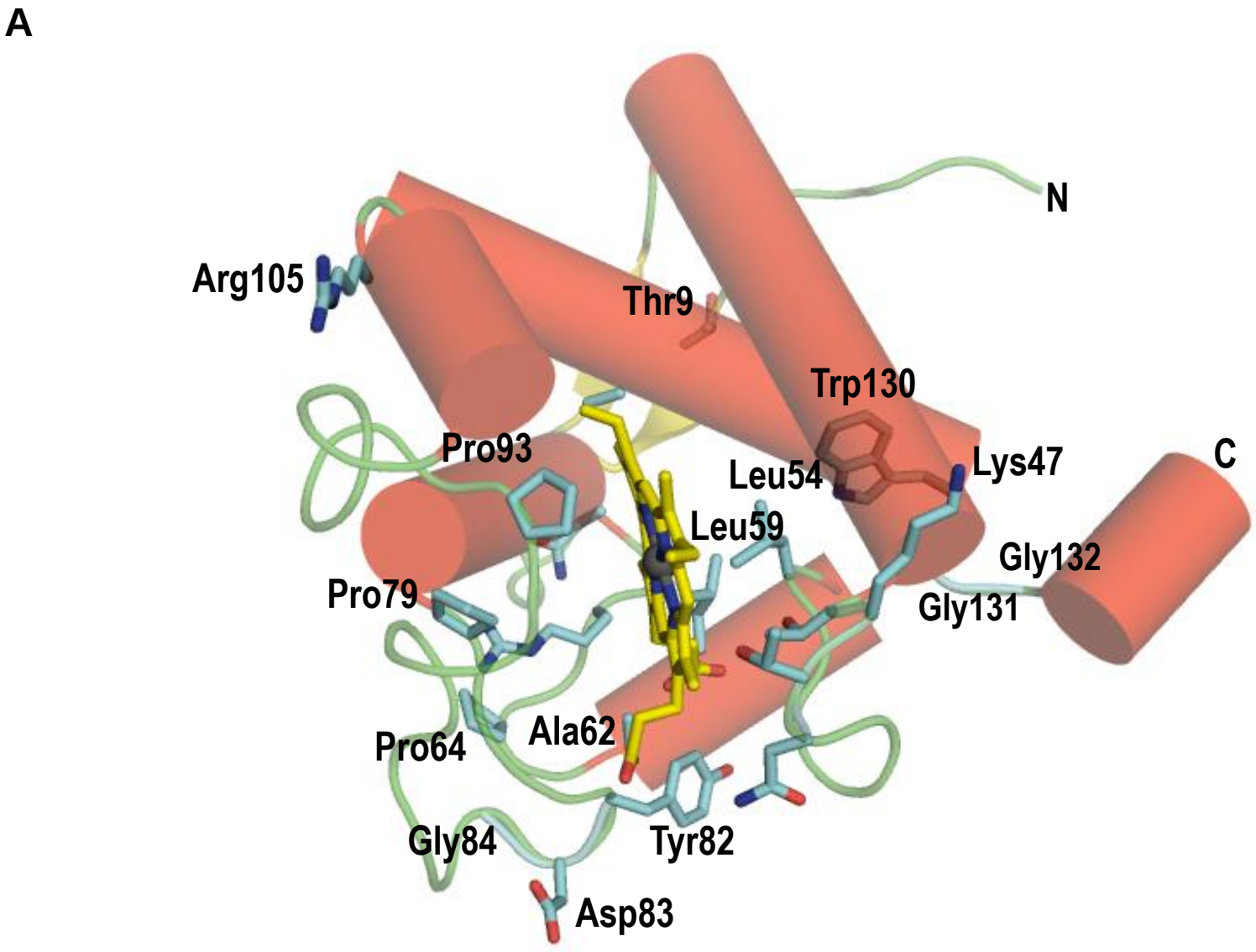
A
N
Arg105
Thr9
Trp130
Pro93
Leu54
Lys47
C
Leu59
Gly132
Pro79
Gly131
Ala62
Pro64
Gly84
Tyr82
Asp83

Figure 4B